# Boosting the Power Grid Resilience to Extreme Weather Events Using Defensive Islanding

Mathaios Panteli, *Member, IEEE*, Dimitris N. Trakas, *Student Member, IEEE*,
Pierluigi Mancarella, *Senior Member, IEEE*, and Nikos D. Hatziargyriou, *Fellow, IEEE*

***Abstract*—Several catastrophic experiences of extreme weather events show that boosting the power grid resilience is becoming increasingly critical. This paper discusses a unified resilience evaluation and operational enhancement approach, which includes a procedure for assessing the impact of severe weather on power systems and a novel risk-based defensive islanding algorithm. This adaptive islanding algorithm aims to mitigate the cascading effects that may occur during weather emergencies. This goes beyond the infrastructure-based measures that are traditionally used as a defense to severe weather. The resilience assessment procedure relies on the concept of fragility curves, which express the weather-dependent failure probabilities of the components. A severity risk index is used to determine the application of defensive islanding, which considers the current network topology and the branches that are at higher risk of tripping due to the weather event. This preventive measure boosts the system resilience by splitting the network into stable and self-adequate islands in order to isolate the components with higher failure probability, whose tripping would trigger cascading events. The proposed approach is illustrated using a simplified version of the Great Britain transmission network, with focus on assessing and improving its resilience to severe windstorms.**

***Index Terms*—Resilience, resiliency, smart grid, defensive islanding, extreme weather, system splitting.**

## I. Introduction

EXTREME weather events can have significant effects on the electrical power critical infrastructures all around the world [1]. For example, when hurricane Sandy hit the United States in 2012, a total of over 8 million customers were left without electricity, with the overall losses in New York and New Jersey exceeding $70 billion. Considering that the frequency and severity of such events is expected to increase in the future as a direct impact of climate change [2], it is becoming more and more critical to develop techniques for evaluating and boosting the resilience of power systems to natural disasters and extreme weather events, in particular.

In the light of natural hazards, it is clear that operating and protecting the power grid from a traditional reliability perspective might not be enough for keeping the lights on. In fact, in addition to being reliable to the most "common" electrical contingencies, power grids need also to be resilient. In the context of power systems, *resilience* can be defined as the grid's ability to withstand extraordinary and high-impact low-probability events that may have never been experienced before, such as extreme weather events, rapidly recover from such disruptive events, and adapt its operation and structure to prevent or mitigate the impact of similar events in the future [3], [4]. A comprehensive framework of power systems resilience is presented and discussed in [5] and [6].

The impact assessment of extreme weather events has attracted the interest of several researchers, such as [7]–[10]. A discussion of the key modeling challenges and limitations of such studies, along with different resilience enhancement measures can be found in [11]. In the existing literature, these measures mainly focus on infrastructure hardening and reinforcement actions, such as building redundant transmission paths or upgrading the power system components with stronger materials. Nevertheless, recent weather-related electrical disturbances evidence that these infrastructure measures may not be always sufficient for keeping the lights on. Hence, they need to be accompanied by the appropriate operational resilience enhancement measures. However, the contribution of operational measures supported by smart grid technologies to power grid resilience during extreme weather events has not been adequately investigated in existing works.

According to the U.S. Department of Energy, a 'smart grid' integrates IT technologies to improve reliability, security and efficiency of the power system [12]. IntelliGrid$^{SM}$, an initiative of the Electric Power Research Institute of USA, is creating the technical foundation for a smart grid and has a vision of a power system able to cope with emergency conditions with self-healing actions by operating in a coordinated, efficient and reliable manner [13]. In this paper, we propose a unified resilience assessment and operational enhancement approach that is well aligned with the above smart grid goals. This approach is composed of a procedure for modelling the impact of weather events on power grids resilience and a defensive islanding algorithm for mitigating the impact of these catastrophic events. This preventive operational action, which is adaptive to the prevailing system and weather conditions

Manuscript received September 1, 2015; revised January 13, 2016; accepted February 20, 2016. Date of publication March 15, 2016; date of current version October 19, 2016. This work was supported in part by the Research Projects Resilient Electricity Networks for Great Britain under Grant EP/I035781/1, and in part by the Autonomic Power Systems under Grant EP/I031650/1. The work of M. Panteli and P. Mancarella was supported by the U.K. Engineering and Physical Science Research Council. Paper no. TSG-01061-2015.

M. Panteli was with the University of Manchester, Manchester M13 9PL, U.K. He is now with the University of Cyprus, Nicosia 1678, Cyprus (e-mail: panteli.mat@gmail.com).

D. N. Trakas and N. D. Hatziargyriou are with the National Technical University of Athens, Athens 157 73, Greece (e-mail: dtrakas@power.ece.ntua.gr; nh@power.ece.ntua.gr).

P. Mancarella is with the University of Manchester, Manchester, U.K. (e-mail: p.mancarella@manchester.ac.uk).

Color versions of one or more of the figures in this paper are available online at http://ieeexplore.ieee.org.

Digital Object Identifier 10.1109/TSG.2016.2535228

by utilizing advanced monitoring capabilities and using real-time data, lies within the smart grid approach for boosting power grid resilience during severe weather, as opposed to the infrastructure resilience measures usually deployed. It therefore provides an insight on the benefits gained by applying smart solutions, which are considered to be less expensive than the infrastructure measures. The application and contribution of islanding schemes has been discussed in several papers [6], [14]–[17].

The resilience assessment procedure presented in this paper is based on Sequential Monte Carlo simulation and is capable of capturing the stochastic and spatiotemporal impact of weather fronts, as they move across transmission networks. It uses the concept of fragility curves, which express the failure probability as a function of weather parameters, e.g., wind speed or snow density. In this work, the application of the defensive islanding solution is determined by a risk-based approach. More specifically, the weather-dependent failure probabilities of the components obtained by the fragility curves are used to identify the most vulnerable components that are at higher risk of tripping due to the weather event. These vulnerable components are used for generating a large number of scenarios (i.e., $2^N$, where $N$ is the number of vulnerable components) that may occur during the weather event. Then, a *Severity Risk Index* (*SRI*) is estimated, which considers the probability and impact of these scenarios. A threshold of *SRI* based on the evolving power system conditions is effectively defined by the proposed method, for which the resilience of the power grid to the extreme weather event benefits from the application of defensive islanding.

The defensive islanding splits the system into stable and self-adequate islands in order to isolate vulnerable components, whose failure would trigger cascading events. Cascading events is the main reason of large blackouts [18] and during extreme weather conditions cascading faults may happen more than five times per day [19]. Defensive islanding can be defined as a graph-cut problem [20]. Here, *constrained spectral clustering* is used to provide an islanding solution that isolates vulnerable components. More details on spectral clustering can be found for instance in [21]–[24].

This paper is structured as follows. Section II discusses the concept of power systems resilience. The proposed approach for assessing and boosting power grid resilience using the proposed defensive islanding algorithm is presented in Section III. In Section IV, this approach is illustrated using a reduced version of the Great Britain transmission network, with focus on the impact of severe wind events. Section V summarizes and concludes the paper.

## II. Power Systems Resilience Conceptual Framework

Fig. 1 shows a conceptual resilience curve that demonstrates the system states during an event, the resilience levels as a function of time with respect to the disturbance event, and the importance of the different resilience features that a system must possess for coping effectively with the evolving conditions associated to an event [5].

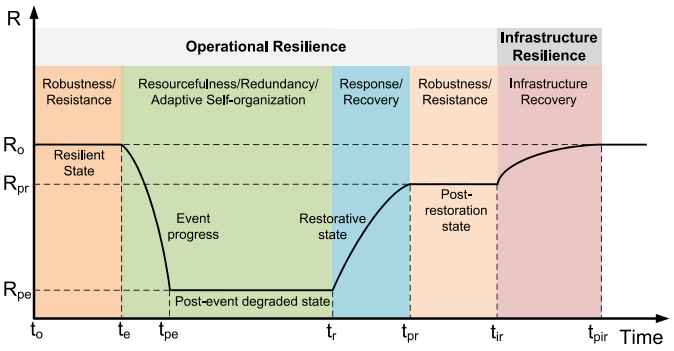


Fig. 1. Conceptual resilience curve associated to an event [5].

Before the event occurs at $t_e (t \in [t_o, t_e])$ the system must be robust enough to withstand the initial shock. Following the event, the system enters the post-event degraded state at $t_{pe}$, with the resilience level decreasing from $R_o$ to $R_{pe}$ (where $R$ is a suitable resilience metric, such as number of customers connected to the system). Resourcefulness, redundancy and self-organization are key resilience features during the event progression ($t \in [t_e, t_{pe}]$), as they provide the control assets to deal with the evolving conditions and mitigate the resilience degradation level, i.e., $R_{pe} - R_o$, before the system restoration is initiated at $t_r$. The post-restoration resilience level, i.e., $R_{pr}$, can be equal to or lower than $R_o$, depending on the effectiveness of the operational actions and on the operational resilience demonstrated by the system during and after the event. Nevertheless, the infrastructure might take longer to be fully restored to its pre-event state, which shows its infrastructure resilience ($t \in [t_{ir}, t_{pir}]$).

Several infrastructure-based measures could be put forward to boost the resilience of power systems in the context of the framework illustrated in Fig. 1 (see for instance the examples in [5] and [11]), including asset reinforcement/hardening solutions and network redundancy. Further, operational solutions based on deployment of Smart Grid technologies can be deployed, which could prove more cost effective for boosting power grid resilience to catastrophic events. In this light, viable options might rely on a mix of preventive and corrective operational measures based on wide area monitoring and control capabilities, which could mitigate the system cascading propagation severity and speed. Defensive islanding (which is the focus of this paper), i.e., controlled splitting of the network into stable islands, can be carried out with limited customer interruptions compared to uncontrolled cascaded events and system splitting, as will be shown later.

## III. Approach for Boosting Resilience Using Defensive Islanding

The need for splitting the network in a controllable way is determined following a risk-based approach. This is used to assess the value of the *SRI* (see below) of the possible scenarios that may occur during the weather event. It also supports the system operators' decision-making as to when to apply the islanding solution for creating stable and sustainable islands and preventing the uncontrollable outage propagation.

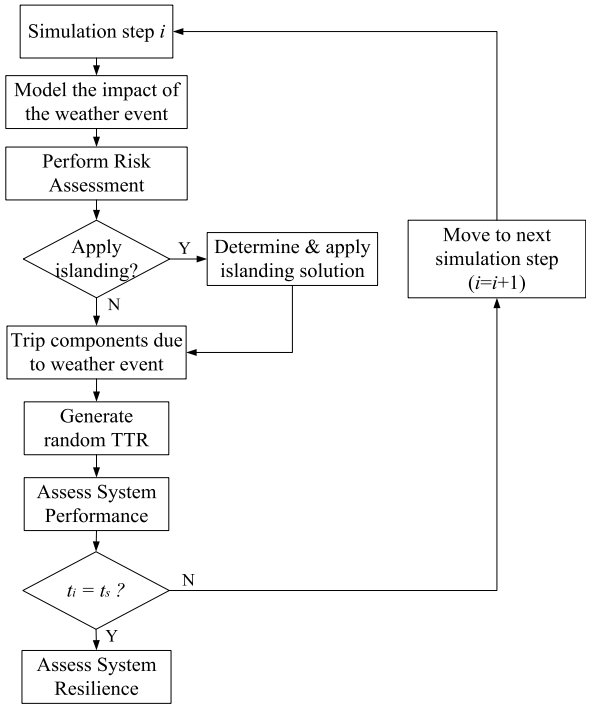


Fig. 2. Flowchart of proposed resilience assessment and operational enhancement procedure using defensive islanding.

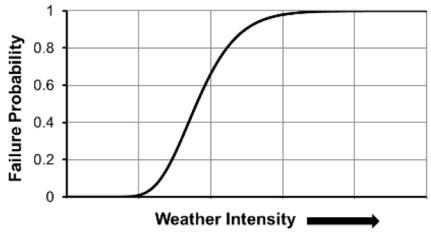


Fig. 3. Generic weather resilience curve related to an individual component.

The proposed approach is composed of the following four main models: (a) assessing the impact of weather events on the power system, (b) risk assessment for determining the *SRI* during the weather event, (c) defensive islanding algorithm for finding the optimal islanding solution, and (d) system resilience assessment with and without the islanding algorithm. Fig. 2 shows the flowchart of the proposed resilience assessment and enhancement procedure.

### A. Modelling the Impact of the Weather Event

The generic fragility curve shown in Fig. 3 relates the failure probability of the components to the weather intensity. Fragility curves have been used in studies where the aim is to assess the impact of a weather event or a natural hazard on the resilience of transmission or distribution networks [25], [26]. At every simulation step, the weather profile (e.g., wind speed or rain intensity) is mapped to these fragility curves for obtaining the weather-dependent failure probabilities of the power system components. This helps determine the system components that are at higher risk of tripping at the next simulation step (i.e., next hour) due to the weather event, which will be used in risk assessment. Here, it is considered that the weather intensity across the power grid can be accurately predicted for the next simulation step. This is acceptable, as in practice the forecasting error for the next hour weather intensity is usually quite low.

By following this approach, the stochastic and spatiotemporal impact of the weather event on the operational state of the individual components is determined.

### B. Risk Assessment

The purpose of risk assessment is to enable informed decisions regarding actions to mitigate risk. In this paper, the risk is introduced by the extreme weather event and the action which will be applied is defensive islanding, in addition to the more traditional actions of generation redispatch to stay within secure network operation following a fault and load shedding as the last resort.

At every simulation step, the failure probabilities estimated in Section III-A are used to determine the vulnerable branches. All the branches having failure probabilities higher than a specified failure probability threshold are considered as vulnerable branches and are used to generate all the possible failure scenarios. More specifically, if the sequence of the contingencies is neglected and the number of vulnerable components is $N$, then the number of possible failure scenarios is $2^N$. From the generated failure scenarios, only those that have higher probability than a pre-specified threshold are selected (i.e., $K$ scenarios). The aforementioned thresholds depend on the system operator and indicate the security criteria to be fulfilled. When determining these thresholds, a trade-off between computational complexity and safety level has to be realized, as the computational complexity increases with the security level due to the higher number of scenarios included in the risk assessment procedure. For example, the lower the failure probability threshold used, the higher the number of vulnerable branches and thus, the number of scenarios to be considered.

Using the impact and probability of the selected failure scenarios, a *Severity Risk Index* (*SRI*) is defined:

$$SRI = \sum_{k=1}^{K} P_k \times Im_k \tag{1}$$

where, $P_k$ is the probability of scenario $k$, $Im_k$ is the impact of scenario $k$ and $K$ the set of selected failure scenarios.

The defensive islanding is applied to prevent or decrease the spread of cascading outages. The *SRI* will be used to help the system operator decide when the defensive islanding should be applied. Here, only the cascading caused by thermal overloads is considered, where a branch will be tripped if its MVA flow violates its short-term emergency rating.

The risk assessment procedure is based on [27]. For a specific weather event:

1) Identify the vulnerable branches.
2) Generate $K$ failure scenarios using the vulnerable branches identified in 1).
3) For each scenario, trip the vulnerable branches and solve the power flow.
4) Identify all branches violating their emergency rating.

5) Remove them and resolve the power flow.
6) Repeat Steps 4) - 5) until one of the following stopping criteria are met:
   (a) No branches are identified in step 4);
   (b) The power flow diverges in steps 3) or 5);
   (c) The procedure exceeds a pre-specified number of iterations of steps 4) and 5).
7) Repeat steps 3) – 6) for each failure scenario.
8) Compute *SRI* according to (1).

The impact of each scenario is considered equal to the amount of load shedding (in MWh) that is carried out for stabilizing the system and depends on the stopping criteria. If the procedure terminates as a result of criterion (b) or (c), it is assumed that the system collapses and the impact of the specific scenario is equal to the total demand. If the procedure stops because of criterion (a), the amount of load that has been shed is recorded. Independent islands may be formed during the risk assessment procedure due to branches failed due to wind or branch overloading. In case a bus is isolated and demand is higher than generation, the appropriate amount of load is shed in order the generation to meet the demand. If the estimated *SRI* (measured in MWh, like the load shedding impact) is larger than the pre-specified threshold $SRI_{thres}$, then the system operator will be notified for activating defensive islanding, as discussed in the next section. The selection of $SRI_{thres}$ is proposed and investigated in Section IV-C.

It should be noted that no operator's actions take place during the risk assessment procedure, and the *SRI* depends on the topology of the system, the loading conditions, the failure probabilities of the branches and the determined thresholds by the system operator.

### C. Defensive Islanding Algorithm

The defensive islanding algorithm is based on constrained spectral clustering which uses power flow data to split the system into islands and isolate the vulnerable components. In the next subsections, the defensive islanding algorithm and constrained spectral clustering are presented.

*1) Defensive Islanding Approach:* Defensive islanding addresses the problem of finding which branches should be disconnected, in order to isolate the vulnerable components and avoid cascading outages. The scheme comprises dynamic preventive control, which is adaptive to the weather conditions and to the various phases of the post-event degraded state (see Fig. 1) at each time step of the simulation, while taking into account the current topology and loading conditions of the system. It is a preventive measure and therefore it is applied to minimize the probability of cascading phenomena.

The topology of network and loading conditions are determined using data reported by PMUs [28]. It is assumed that PMUs, distributed throughout the network, check the connectivity of the network branches and measure the branches' flow values, which are transferred to a central controller through advanced communication technologies. The full observability of the system can be achieved placing PMUs in about one third of the buses, and in the case this number of PMUs is not available, a combination of PMU and SCADA measurements are used for state estimation [29]. The PMUs' measurements are also used for the reconnection of the islands. Frequency, voltage and phase angle conditions must be satisfied for the reconnection and thus monitoring is critical. The PMUs' real-time measurements are used to adjust the frequency, voltage and phase angle of islands to meet the requirements of synchronization [30].

The isolation of vulnerable branches leads to the isolation of vulnerable buses to which the vulnerable branches are connected. The formed islands and their number depend on the geographical location of the vulnerable buses, as well as the current topology of the system at each simulation step. These islands operate as independent systems and load shedding is carried out, if necessary, in order to form islands that satisfy steady state constraints. The proposed method aims to isolate the vulnerable buses in one island, since the bigger is the island the stronger it is against the branches' failure. Furthermore, the isolation of vulnerable buses in more than one island may lead to load shedding increase due to congestions.

An islanding solution with minimal power flow disruption is assumed to minimize load shedding. According to [21], minimal power flow disruption creates islands with the minimum change from the pre-disturbance power-flow pattern. This property of the objective function has also minimum impact on the transient stability of the islands, reduces the possibility of overloading the transmission lines within the island, and facilitates the islands eventual reintegration with the rest of the system.

To create stable islands, the islanding solution must satisfy steady state and dynamic constraints, such as load generation balance, thermal limits, and transient and voltage stability. It is beyond the scope of this paper however to find a solution that satisfies all constraints. The proposed islanding method is focused in creating islands that satisfy steady state constraints. By satisfying these constraints and considering the benefits of minimal power flow disruption, it is assumed that the islands are also stable, thus transient and voltage stability of the islands after a contingency are not examined.

Based on the above, defensive islanding can be defined as a graph-cut problem and constrained spectral clustering is used to provide a solution. The theoretical background of constrained spectral clustering is given in the next section.

*2) Constrained Spectral Clustering Background:* The power system can be described by an undirected graph $G(V, E, W)$ with vertex set $V$ (buses) and edge set $E$ (branches). The matrix $W$ is the weighted adjacency matrix and must satisfy the following properties: $w_{ij} = w_{ji}$, $w_{ii} = 0$ and $w_{ij} = 0$, if vertex $i$ is not adjacent to vertex $j$ in $G$. The apparent power flow of the branches is used to define matrix $W$ and the weight $w_{ij}$ is defined as:

$$w_{ij} = \frac{|S_{ij}| + |S_{ji}|}{2} \tag{2}$$

where, $S_{ij}$ is the apparent power flow from bus $i$ to $j$ [19], [22].

The constrained spectral clustering is based on the Laplacian matrix. There are two main types of Laplacian matrices, namely, normalized and unnormalized [31]. The normalized one performs better for clustering techniques [22], [32] and is

defined as:

$$L_n = I - D^{-1/2} W D^{-1/2} \tag{3}$$

where, $I$ is the identity matrix and $D$ is the diagonal degree matrix with the degrees of vertices on the diagonal. The degree $d_i$ of a vertex $v_i \in V$ sums the weights of all edges adjacent to $v_i$ and is defined as [24]:

$$d_i = \sum_{j=1}^{N_V} w_{ij} \tag{4}$$

where, $N_V$ is the number of vertices. Constrained spectral clustering is applied to set as constraint all the vulnerable buses to be included in the same island. Assuming the first $s$ buses are those that have to be isolated and $n$ is the total number of the buses (also matrices $D$ and $W$ need to be sorted in the same way), the constraints can be introduced using a constraint matrix $C$ [21], [33]:

$$C = \begin{bmatrix} 1_{s\times 1} & 0_{s\times(n-s)} \\ 0_{(n-s)\times 1} & I_{(n-s)\times(n-s)} \end{bmatrix} \tag{5}$$

where $I$ is the identity matrix, 0 is the null matrix and 1 is the matrix full of ones. Therefore, the matrix $C$ has dimensions $n \times (n - s + 1)$ as the must-link buses (i.e., vulnerable buses) are represented by one equivalent bus.

The eigenvectors $u_1$ and $u_2$ corresponding to the two smallest eigenvalues of the generalized eigen-problem $C^T L_n C u = \lambda C^T C u$ are then computed, where $\lambda$ is the eigenvalue associated with eigenvector $u$.

Next, the computed eigenvectors are normalized to have length 1 in $\mathbb{R}^2$, so that:

$$u_i^{'} = \frac{u_i}{\|u_i\|}, \quad i = 1, 2 \tag{6}$$

The vectors $Cu_1^{'}$ and $Cu_2^{'}$ are used as coordinates of the vertices in $\mathbb{R}^2$. The vertices are clustered using hierarchical clustering [32].

Eventually, the constrained spectral clustering provides a solution that minimizes power flow disruption and divides the power system into two subsets $V_1$ and $V_2$. Assuming that vulnerable buses belong to $V_1$, the quality of the islanding solution is defined as the ratio of the number of vulnerable buses to the total number of buses in $V_1$. If the ratio is smaller than a desired value, the constrained spectral clustering is reapplied in $V_1$. The same procedure is repeated until the quality of the islanding solution is considered satisfactory and the branches that should be disconnected to form the islands are those obtained from the last application of constrained spectral clustering. The quality of an islanding solution takes values in the range [0, 1]. Large values limit the possible formations of islands, while low values means that the formed island with vulnerable buses could include a higher number of non-vulnerable buses than the vulnerable ones. After exhaustive tests performed offline, the minimum desired ratio has been selected equal to 67% ($2/3 = 0.67$) in this study. The network may be divided into islands due to branches' failures caused by extreme weather. In this case, each island is treated as an independent system and the network may be divided in more than two islands.

### D. System Resilience Assessment

After applying the appropriate islanding solution, the next step is to determine which components will actually trip due to the weather event. To do this, the weather-dependent failure probabilities obtained by the fragility curves are compared with a uniformly distributed random number $r \sim U(0, 1)$. If the failure probability of the component is larger than $r$, then it is tripped. This is a particularly useful approach in weather- and natural hazard-related studies (e.g., [34], [35]) for determining the status of the components at each simulation step. Once a component outage occurs, the time to repair (*TTR*) is randomly generated following an exponential distribution. In order to capture the increasing *TTR* for higher component damage as a result of weather events with higher intensity, the *TTR* under normal weather is multiplied with a uniformly distributed random number within a pre-determined range (as will be discussed in later sections).

The system performance is then evaluated at every simulation step. This helps determine if load has to be shed for balancing the network. This procedure is repeated until the end of the simulation ($t_s$) is reached. The system resilience is then assessed, which can be expressed by the number of customers disconnected during the weather event.

The simulation procedure of Fig. 2 is conducted with and without considering defensive islanding. This determines the contribution of this preventive control action to the resilience of the power system during weather emergencies.

## IV. Case Study Application

This section presents the results of the proposed approach applied to a simplified 29-bus version of the Great Britain (GB) transmission network. A simulation period of one winter week is used, where the peak demand and high wind speeds are usually observed in GB. Further, an hourly resolution is used, which is considered adequate for modelling weather events. An adequate number of scenarios has been considered in the simulations (as shown in Section IV-C) to ensure the accuracy of the methodology.

### A. Test Network and Weather Regions

The simplified GB transmission network used in this study is shown in Fig. 4.a [36]. This model consists of 29 buses; 98 overhead transmission lines in double circuit configuration and one single circuit transmission line (i.e., between nodes 2 and 3); and 65 generators of different technologies (e.g., wind, nuclear and CCGT) located at 24 nodes, of total installed capacity of around 80GW. The hourly node demand has been obtained by the 2011 Seven Years Statement, National Grid [37] with a peak network demand of about 56GW. This is considered independent from the evolving weather conditions.

In order to account for the spatial impact of the windstorm across the transmission network, the test network has been arbitrarily divided in 6 weather regions, as shown in Fig. 4.b. MERRA re-analysis [38] has been used for obtaining the wind profiles at the different locations in GB. Weather conditions are assumed to be homogenous within each weather region. The components within each region are thus exposed

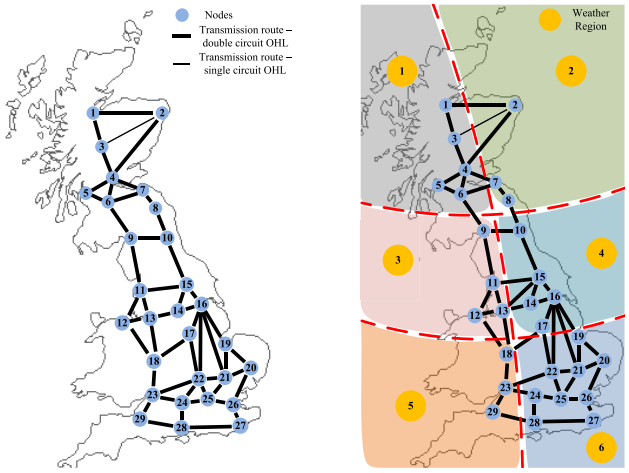


a) Simplified GB network b) Weather regions

Fig. 4. The simplified 29-bus GB transmission network.

to the same wind conditions, which means that the fragility of the components is the same within each region. As the wind data obtained by MERRA re-analysis represent hourly average wind speeds, the data used in the simulations have been scaled-up in order to model severe windstorms that can be a threat to the network resilience. In particular, windstorms with maximum wind speeds up to 46m/s have been simulated, which represent wind speeds experienced during hurricanes based on the Beaufort wind scale provided by Met Office, U.K. [39] and are similar to the ones occurred in the worst historical windstorms in U.K. [40]. Further, according to hourly maximum gust speeds recorded in severe historical windstorms in GB [40], [41], it is observed that the regions in North GB are the ones hit harder and more frequently by windstorms. Therefore, this analysis focuses on simulating windstorms occurring in weather regions 1 and 2 of Fig. 4.b.

### B. Simulation Data

The application of the proposed framework focuses on the impact of severe windstorms on the transmission lines and towers. Fig. 5 shows the wind fragility curves used. The tower wind fragility curve is an example of the curves generated from the 'Resilient Electricity Networks for Great Britain (RESNET)' project [10] and refers to the most typical steel transmission tower in GB transmission network. It is assumed that there is one tower every 300m and that they are connected in series, so collapse of a single tower trips the transmission corridor. The transmission line fragility curve is assumed here for demonstration purposes. The pick-up wind speed of this curve (i.e., approximately 30m/s) is in line with a statistical study performed in [42], which relates the transmission lines' failure probability in GB to wind speeds. A transmission corridor can thus trip due to a tower collapse, or a line (conductor) failure, e.g., shackle failure. It has to be noted that these fragility curves refer to the independent collapse of a single transmission tower and to the failure of a transmission line as one (i.e., not to the line spans between the transmission towers), respectively.

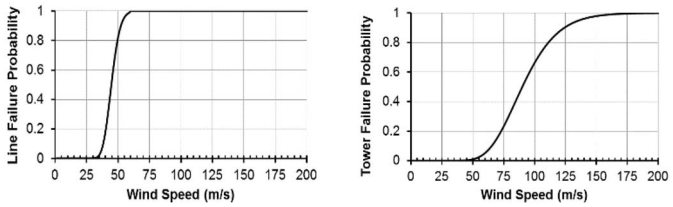


a) Line fragility curve b) Tower fragility curve

Fig. 5. Wind fragility curves.

The probability of branch *br* to trip due to wind is defined as:

$$P_{br}(w) = P_{br,B}(w) + P_{br,T}(w) - P_{br,B}(w)P_{br,T}(w) \quad (7)$$

where, $P_{br}(w)$ is the probability of branch *br* to fail as a function of wind speed ($w$), and $P_{br,B}(w)$ and $P_{br,T}(w)$ are the probabilities of branch *br* to fail due to branch and tower trip, respectively. Probability $P_{br,B}(w)$ is obtained by the fragility curve of Fig. 5.a. Considering that the transmission towers fail independently of one another and that the individual failure probabilities are the same, $P_{br,T}(w)$ is given as follows:

$$P_{br,T}(w) = 1 - \left(1 - P_{T\_ind}(w)\right)^{N_T} \quad (8)$$

where, $P_{T\_ind}(w)$ is the individual tower failure probability as obtained by the fragility curve of Fig. 5.b and $N_T$ is the number of towers across branch *br* (assumed one tower every 300m). $P_{br}(w)$ is used to determine the vulnerable branches, i.e., the ones that are at high risk of tripping in the next simulation step due to the windstorm. If $P_{br}(w)$ is higher than the specified threshold, the branch *br* is considered as vulnerable and included in the generation of the possible failure scenarios.

The lines and towers *TTR* under normal weather (i.e., $TTR_{normal}$) are assumed 10hrs and 50hrs respectively. As aforementioned, a way of modelling the increasing impact of windstorms with higher intensity on $TTR_{normal}$ is to multiply $TTR_{normal}$ with a uniformly distributed random number $h$ in a pre-determined range (i.e., $h \sim U[x_1, x_2]$). In this application, the range $[x_1, x_2]$ is [2, 4] for wind speeds up to 40m/s and [5,7] for higher wind speeds. Therefore, for example, a restoration of a transmission tower can last from a couple of days to more than a week depending on the damage by the windstorm. If information on the restoration performance of the electrical utility during weather emergencies is available, then more accurate restoration models can be built.

### C. Simulation Results

As mentioned in Section IV-A, during the simulations the weather regions 1 and 2 of Fig. 4.b are subject to windstorms while in the rest of the system it is assumed that there are no high wind speeds and the normal failure probability of branches is 1%. Each branch with a failure probability $P_{br}(w)$ higher than 1% is considered vulnerable and is used to generate the examined failure scenarios. It is also worth noting that the failure probabilities of the branches labelled as vulnerable are significantly higher than the failure probabilities of the branches classified as non-vulnerable. Therefore, the sampling of the fragility curves using the evolving wind conditions

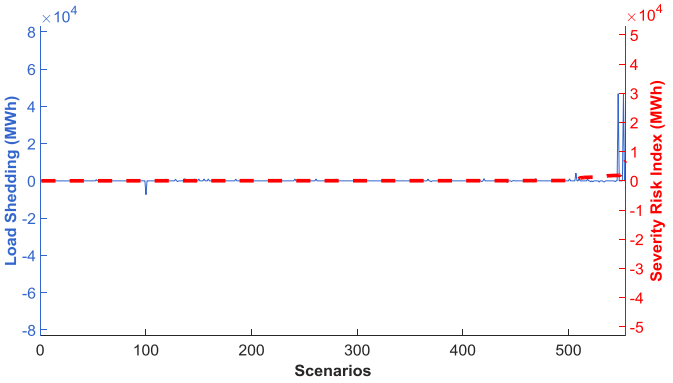


Fig. 6. *SRI* and corresponding difference of load shedding without and with defensive islanding for maximum wind speed of 36m/s.

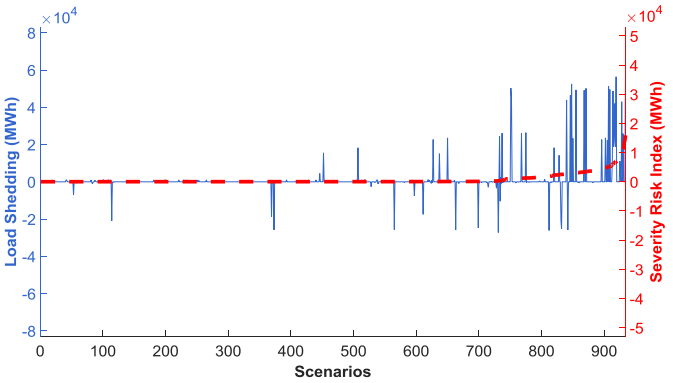


Fig. 7. *SRI* and corresponding difference of load shedding without and with defensive islanding for maximum wind speed of 38m/s.

within the time-series for determining their failure probabilities at each simulation step allows the systematic quantification of the spatio-temporal impact of the windstorm on the individual components, and in turn on the risk and resilience of the whole system. The failure scenarios considered in the risk assessment procedure have a probability to occur higher than 1%. These thresholds are selected equal to the normal failure probability of branches in order to examine a large number of scenarios and to draw conclusions for a wide range of wind speeds.

Figs. 6-11 show the *SRI* (red dashed line) and the corresponding difference of load shedding that is carried out without and with defensive islanding for a range of maximum wind speeds that may occur in the affected areas. Every simulation step where $SRI>0$ (i.e., probability and impact higher than zero) is treated as a scenario under investigation.

Those scenarios are presented in ascending order according to their *SRI* values. When the difference of load shedding is positive, the load that needs to be shed when applying defensive islanding is reduced. Consequently, it is beneficial to apply defensive islanding as a preventive control method. Conversely, when the difference of load shedding is negative, load shedding increases when defensive islanding is applied. It can be observed that with higher wind speeds the number of the scenarios under investigation increases. Additionally, the

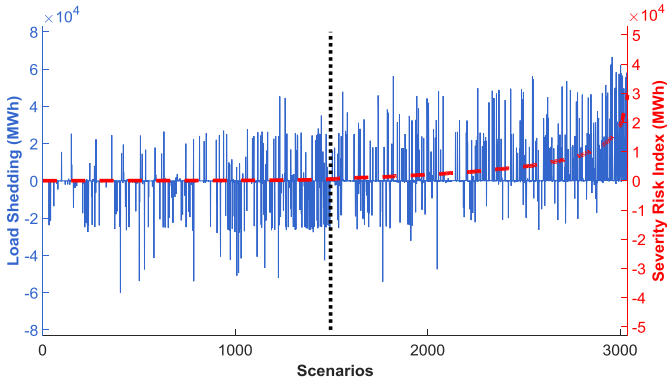


Fig. 8. *SRI* and corresponding difference of load shedding without and with defensive islanding for maximum wind speed of 40m/s.

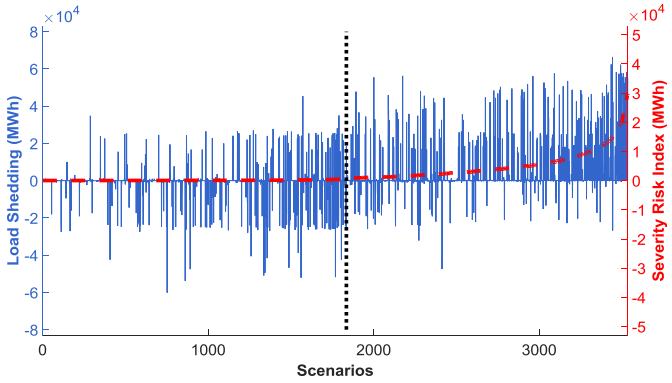


Fig. 9. *SRI* and corresponding difference of load shedding without and with defensive islanding for maximum wind speed of 42m/s.

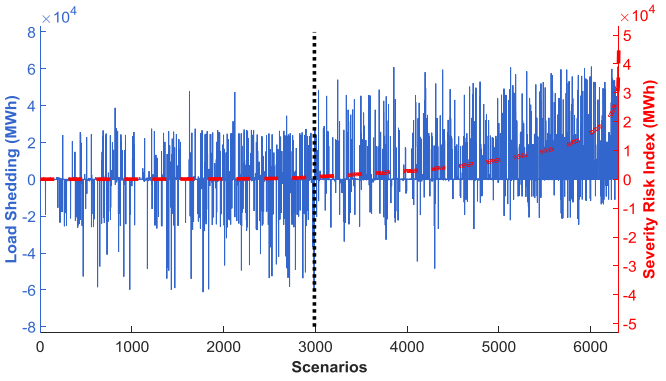


Fig. 10. *SRI* and corresponding difference of load shedding without and with defensive islanding for maximum wind speed of 44m/s.

percentage of scenarios with a positive load shedding difference increases with the increase in *SRI*: this shows that for higher *SRI* values the network resilience benefits from defensive islanding.

By comparing Figs. 6-11, it can be observed that for wind speeds up to 36m/s (Fig. 6), the system can effectively withstand the stress imposed by the windstorm. Therefore, defensive islanding has limited value. For maximum wind speeds of 38m/s (Fig. 7), defensive islanding could potentially be beneficial, but proper conclusions cannot be drawn due to the low number of scenarios. For wind speeds higher than

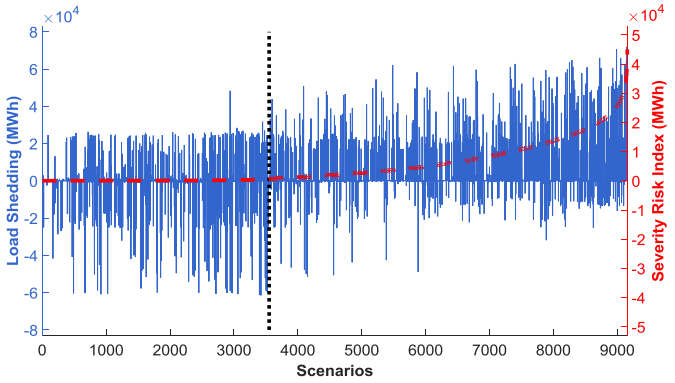


Fig. 11. *SRI* and corresponding difference of load shedding without and with defensive islanding for maximum wind speed of 46m/s.

38m/s, the resilience of the test system is significantly compromised, as shown by the large number of scenarios where load shedding takes place.

The proper selection of $SRI_{thres}$ for online applications requires extensive offline studies. Based on simulation results, it is possible to define the $SRI_{thres}$, for which defensive islanding is applied, as the value that maximizes the function $F$:

$$F = \sum_{S^*} (LS - LS_{DI}) \tag{9}$$

where $S^*$ is the set of all the scenarios with *SRI* values higher than the selected $SRI_{thres}$. The *LS* and $LS_{DI}$ are the MWh amount of load shedding which is carried out without and with defensive islanding, respectively.

The *SRI* value, marked with the black dotted line in Figs. 8-11 represents the $SRI_{thres}$. It is noted that when defensive islanding is applied, the load that is shed in order to form stable and self-adequate islands is included in the overall load shedding $LS_{DI}$.

Table I shows the $SRI_{thres}$ and the maximum *SRI* values for each windstorm intensity investigated in this study. It can be observed that the maximum *SRI* is getting larger values with the increase in wind speed. Furthermore, $SRI_{thres}$ takes similar values in all the range of maximum wind speeds, given that *SRI* takes values in the range $[0, 4.5 \cdot 10^4]$ MWh. For a real life application, a single characteristic threshold within the range of those $SRI_{thres}$ could be defined. Table II presents the value of function $F$ considering all the combinations of maximum wind speeds and $SRI_{thres}$. The mean value of the $SRI_{thres}$ values of the different wind speeds is also used. The results in Table II demonstrate that the selection of any of these values as the characteristic threshold of the test system leads to similar results. In addition it is observed that as the wind speed increases, defensive islanding leads to higher values of function $F$.

In Figs. 8-11, it can be seen that for $SRI > SRI_{thres}$, defensive islanding benefits the network resilience (i.e., load shedding>0) in the majority of the scenarios. Moreover, defensive islanding seems beneficial in a number of scenarios for *SRI* lower than $SRI_{thres}$. This observation is summarized in

TABLE I
DEFINED $SRI_{thres}$ AND $SRI_{max}$ FOR A RANGE OF MAXIMUM WIND SPEEDS

| Maximum Wind Speed (m/s) | $SRI_{thres}$ (MWh) | $SRI_{max}$ (MWh) |
|---|---|---|
| **36** | - | $0.68 \cdot 10^4$ |
| **38** | - | $1.61 \cdot 10^4$ |
| **40** | 597.13 | $2.94 \cdot 10^4$ |
| **42** | 583.50 | $2.97 \cdot 10^4$ |
| **44** | 866.76 | $4.47 \cdot 10^4$ |
| **46** | 673.71 | $4.50 \cdot 10^4$ |

TABLE II
FUNCTION $F$ FOR ALL THE COMBINATIONS OF WIND SPEEDS AND $SRI_{thres}$

| $SRI_{thres}$ (MWh) | Maximum Wind Speed (m/s) | | | |
|---|---|---|---|---|
| | **40** | **42** | **44** | **46** |
| | $F$ (MWh·10^6) | | | |
| **597.13** | 5.589 | 6.985 | 11.912 | 14.206 |
| **583.50** | 5.588 | 7.004 | 11.937 | 14.223 |
| **866.76** | 5.565 | 6.933 | 12.102 | 14.118 |
| **673.71** | 5.573 | 6.981 | 12.070 | 14.310 |
| **Mean Value (680.28)** | 5.580 | 6.959 | 12.015 | 14.164 |

TABLE III
STATISTICAL ANALYSIS OF THE SIMULATION RESULTS

| Max Wind Speed (m/s) | $LS < LS_{DI}$ (%) | $LS > LS_{DI}$ (%) | $LS = LS_{DI} = 0$ (%) | $LS = LS_{DI} > 0$ (%) |
|---|---|---|---|---|
| **40** | 25.95 | 20.54 | 43.95 | 9.56 |
| | 18.96 | 46.34 | 18.71 | 15.99 |
| **42** | 23.91 | 24.57 | 40.03 | 11.49 |
| | 18.17 | 49.15 | 16.49 | 16.19 |
| **44** | 22.79 | 27.38 | 35.27 | 14.56 |
| | 15.19 | 55.77 | 10.30 | 18.74 |
| **46** | 21.01 | 32.34 | 28.51 | 18.14 |
| | 13.93 | 64.27 | 5.61 | 16.19 |

Table III, which shows the statistical analysis of the simulation results (in percentage of the total scenarios considered in the analysis). The shaded and unshaded rows of Table III refer to *SRI* values lower and higher than the $SRI_{thres}$, respectively. The second and third columns is the percentage of the number of scenarios where *LS* is lower and higher than $LS_{DI}$, respectively. The fourth column is the percentage of scenarios where load shedding is not needed with or without defensive islanding. The fifth column is the percentage of scenarios, where the load shedding with and without defensive islanding is equal and higher than zero. In these scenarios the load shedding that is carried out in both cases is due to bus isolation after the uncontrolled outage of branches.

As can be seen from Table III, for $SRI > SRI_{thres}$ (i.e., unshaded rows) the percentage of the scenarios where the defensive islanding is beneficial, i.e., $LS > LS_{DI}$, increases with the wind speed from 46.34% for 40m/s to 64.27% for 46m/s. Further, it is more than double (i.e., approximately 4.5 times larger for maximum wind speed of 46m/s) than the percentage of cases where the defensive islanding results in higher load shedding (i.e., $LS < LS_{DI}$) for all the wind speeds. In contrast, for $SRI < SRI_{thres}$ this difference is much smaller. Therefore, this analysis shows that defensive islanding is beneficial when

the risk of losing customers is high, which might be the case during severe windstorms.

## V. Conclusions

This paper has presented an approach for boosting the resilience of power grids to extreme weather events using a smart operational resilience measure, i.e., defensive islanding. This provides insights on the contribution of smart measures to power grid resilience, in contrast to different hardening infrastructure measures usually deployed.

The proposed approach has been illustrated through the impact assessment of windstorms on a simplified version of the Great Britain transmission network. The wind-dependent failure probabilities were obtained using fragility curves, which are then used for generating a large number of possible failure scenarios that could occur during the windstorm. Following a risk-based approach and the conduction of several offline studies, a threshold of a severity risk index (*SRI*) has been defined, for which power grid resilience benefits from the application of dynamic defensive islanding. The analysis has been conducted for a wide range of windstorm intensities to determine when the application of defensive islanding benefits power grid resilience. It has effectively been demonstrated that the application of the defensive islanding becomes increasingly beneficial for high *SRI* values (i.e., $SRI > SRI_{thres}$), whereby the threat of uncontrollable cascading failures and customer disconnection is relatively high.

The $SRI_{thres}$ defined in this paper can support the decision-making of the system operator on when to apply the defensive islanding during online applications. This is critically important as it provides the operators with an additional operational measure for dealing with the prevailing weather conditions and contributes significantly to the management of natural disasters. The proposed methodology can also be applied to any weather event (e.g., floods), provided that the relevant information is available, e.g., fragility curves. Further, the methodology is of general validity, and a higher time resolution (i.e., $<$1hr) could possibly be used for the cascading modelling during the weather event. This would increase the accuracy of the proposed model, but requires that the relevant weather data are available at the desired resolution in order to ensure consistency between the modelling of the electrical cascading and of the impact of the weather front moving across the network.

## References


[1] P. SouthWell, "Disaster recovery within a cigre strategic framework: Network resilience, trends and areas of future work," CIGRE Study Committee C1, Aug. 2014.

[2] President's Council of Economic Advisers, "Economic benefits of increasing electric grid resilience to weather outages," Executive Office President, U.S. Dept. Energy, Office of Elect. Del. Energy Rel., Washington, DC, USA, Tech. Rep., Aug. 2013.

[3] A. R. Berkeley, III and M. Wallace, "A framework for establishing critical infrastructure resilience goals: Final goals and recommendations," Nat. Infrastruct. Advisory Council (NIAC), Washington, DC, USA, Oct. 2010.

[4] M. Chaudry *et al.*, *Building a Resilient UK Energy System*. London, U.K.: UK Energy Res. Centre, Apr. 2011.

[5] M. Panteli and P. Mancarella, "The grid: Stronger, bigger, smarter?: Presenting a conceptual framework of power system resilience," *IEEE Power Energy Mag.*, vol. 13, no. 3, pp. 58–66, May/Jun. 2015.

[6] Y. Wang, C. Chen, J. Wang, and R. Baldick, "Research on resilience of power systems under natural disasters—A review," *IEEE Trans. Power Syst.*, vol. 31, no. 2, pp. 1604–1613, Mar. 2016.

[7] M. R. Bhuiyan and R. N. Allan, "Inclusion of weather effects in composite system reliability evaluation using sequential simulation," *IEE Proc. Gener. Transm. Distrib.*, vol. 141, no. 6, pp. 575–584, Nov. 1994.

[8] R. Billinton and G. Singh, "Application of adverse and extreme adverse weather: Modelling in transmission and distribution system reliability evaluation," *IET Gener. Transm. Distrib.*, vol. 153, no. 1, pp. 115–120, Jan. 2006.

[9] L. Yong and C. Singh, "A methodology for evaluation of hurricane impact on composite power system reliability," *IEEE Trans. Power Syst.*, vol. 26, no. 1, pp. 145–152, Feb. 2011.

[10] M. Panteli and P. Mancarella, "Modeling and evaluating the resilience of critical electrical power infrastructure to extreme weather events," *IEEE Syst. J.*, pp. 1–10, Feb. 2015.

[11] M. Panteli and P. Mancarella, "Influence of extreme weather and climate change on the resilience of power systems: Impacts and possible mitigation strategies," *Elect. Power Syst. Res.*, vol. 127, pp. 259–270, Oct. 2015.

[12] U.S. Department of Energy, "Smart Grid System Report," SEC. 1302., Washington, DC, USA, Jul. 2009.

[13] J. B. Ekanayake, *Smart Grid: Technology and Applications*. Hoboken, NJ, USA: Wiley, 2012.

[14] Z. Wang and J. Wang, "Self-healing resilient distribution systems based on sectionalization into microgrids," *IEEE Trans. Power Syst.*, vol. 30, no. 6, pp. 31–39, Nov. 2015.

[15] M. Vaiman *et al.*, "Risk assessment of cascading outages: Methodologies and challenges," *IEEE Trans. Power Syst.*, vol. 27, no. 2, pp. 631–641, May 2012.

[16] M. Amin, "Challenges in reliability, security, efficiency, and resilience of energy infrastructure: Toward smart self-healing electric power grid," in *Proc. IEEE Power Energy Soc. Gen. Meeting Convers. Del. Elect. Energy 21st Century*, Pittsburgh, PA, USA, 2008, pp. 1–5.

[17] L. R. Phillips *et al.*, "Agents and islands: Managing a power system before, during, and after transition to the islanded state," in *Proc. Int. Conf. Syst. Syst. Eng. (IEEE/SMC)*, Los Angeles, CA, USA, 2006, pp. 161–166.

[18] D. P. Nedic, I. Dobson, D. S. Kirschen, B. A. Carreras, and V. E. Lynch, "Criticality in a cascading failure blackout model," *Elect. Power Energy Syst.*, vol. 28, no. 9, pp. 627–633, 2006.

[19] D. Xianzhong and S. Sheng, "Self-organized criticality in time series of power systems fault, its mechanism, and potential application," *IEEE Trans. Power Syst.*, vol. 25, no. 4, pp. 1857–1864, Nov. 2010.

[20] R. Moreno and A. Torres, "Security of the power system based on the separation into islands," in *Proc. IEEE PES Conf. Innov. Smart Grid Technol. (ISGT Latin America)*, Medellin, Colombia, 2011, pp. 1–5.

[21] L. Ding, F. M. Gonzalez-Longatt, P. Wall, and V. Terzija, "Two-step spectral clustering controlled islanding algorithm," *IEEE Trans. Power Syst.*, vol. 28, no. 1, pp. 75–84, Feb. 2013.

[22] J. Quirós-Tortós, R. Sánchez-García, J. Brodzki, J. Bialek, and V. Terzija, "Constrained spectral clustering-based methodology for intentional controlled islanding of large-scale power systems," *IET Gener. Transm. Distrib.*, vol. 9, no. 1, pp. 31–42, Jan. 2015.

[23] D. N. Trakas, E. M. Voumvoulakis, and N. D. Hatziargyriou, "Decentralized control of power system zones based on probabilistic constrained load flow," in *Proc. Int. Conf. Probabilistic Methods Appl. Power Syst. (PMAPS)*, Durham, NC, USA, 2014, pp. 1–6.

[24] H. Mehrjerdi, S. Lefebvre, M. Saad, and D. Asber, "A decentralized control of partitioned power networks for voltage regulation and prevention against disturbance propagation," *IEEE Trans. Power Syst.*, vol. 28, no. 2, pp. 1461–1469, May 2013.

[25] N. R. Romero, L. K. Nozick, I. D. Dobson, X. Ningxiong, and D. A. Jones, "Transmission and generation expansion to mitigate seismic risk," *IEEE Trans. Power Syst.*, vol. 28, no. 4, pp. 3692–3701, Nov. 2013.

[26] Department of Homeland Security Emergency Preparedness and Response Directorate, *Multi-Hazard Loss Estimation Methodology Earthquake Model (HAZUS MR4)*, Fed. Emergency Manage. Agency, Washington, DC, USA, 2003.

[27] M. Ni, J. D. McCalley, V. Vittal, and T. Tayyib, "Online risk-based security assessment," *IEEE Trans. Power Syst.*, vol. 18, no. 1, pp. 258–265, Feb. 2003.

[28] A. Ashrafi and S. M. Shahrtash, "Dynamic wide area voltage control strategy based on organized multi-agent system," *IEEE Trans. Power Syst.*, vol. 29, no. 6, pp. 2590–2601, Nov. 2014.
[29] F. Raak, Y. Susuki, and T. Hikihara, "Data-driven partitioning of power networks via Koopman mode analysis," *IEEE Trans. Power Syst.*, pp. 1–10, Sep. 2015.
[30] Z. Qin, S. Liu, and Y. Hou, "Virtual synchroscope: A novel application of PMU for system restoration," in *Proc. Int. Conf. Adv. Power Syst. Automa. Protect. (APAP)*, Beijing, China, 2011, pp. 193–197.
[31] U. von Luxburg, "A tutorial on spectral clustering," *Stat. Comput.*, vol. 17, no. 4, pp. 395–416, 2007.
[32] R. J. Sanchez-Garcia *et al.*, "Hierarchical spectral clustering of power grids," *IEEE Trans. Power Syst.*, vol. 29, no. 5, pp. 2229–2237, Sep. 2014.
[33] T. De Bie, J. Suykens, and B. De Moor, "Learning from general label constraints," in *Structural, Syntactic, and Statistical Pattern Recognition*. Berlin, Germany: Springer-Verlag, 2004, pp. 671–679.
[34] M. Ouyang and L. Dueñas-Osorio, "Time-dependent resilience assessment and improvement of urban infrastructure systems," *Chaos*, vol. 22, no. 3, 2012, Art. no. 033122.
[35] J. Winkler, L. Dueñas-Osorio, R. Stein, and D. Subramanian, "Performance assessment of topologically diverse power systems subjected to hurricane events," *Rel. Eng. Syst. Safety*, vol. 95, no. 4, pp. 323–336, 2010.
[36] M. Belivanis and K. Bell, "Representative GB network model: Notes," Univ. Strathclyde, Glasgow, U.K., Apr. 2011.
[37] *2011 National Electricity Transmission System (NETS) Seven Year Statement*, National Grid PLC, Warwick, U.K., 2011.
[38] (Mar. 2015). *MERRA Re-Analysis*. [Online]. Available: http://gmao.gsfc.nasa.gov/.
[39] U.K. Met Office. (Jul. 2015). *Beaufort Wind Force Scale*. [Online]. Available: http://www.metoffice.gov.uk/guide/weather/marine/beaufort-scale.
[40] U.K. Met Office. (Mar. 2015). *Met Office Integrated Data Archive System (MIDAS)*. [Online]. Available: http://catalogue.ceda.ac.uk/uuid/245df050d5_7a500c183b88df509f5f5a.
[41] European Centre for Medium-Range Weather Forecasts. (Mar. 2015). *ERA Interim*. [Online]. Available: http://apps.ecmwf.int/datasets/data/interim-full-daily/.
[42] K. Murray and K. R. W. Bell, "Wind related faults on the GB transmission network," in *Proc. Probabilistic Methods Appl. Power Syst. (PMAPS)*, Durham, U.K., 2014, pp. 1–6.

**Mathaios Panteli** (S'09–M'13) received the MEng degree in Electrical and Computer Engineering from Aristotle University of Thessaloniki, Greece in 2009 and the PhD degree in Electrical Power Engineering from The University of Manchester, UK in 2013. After a few years as a Post-doctoral Research Associate at The University of Manchester, he joined University of Cyprus in September 2015, where he is currently a Research Associate. His main research interests include analysis and prevention of power system blackouts, situation awareness in power systems and resilience assessment of power systems to natural hazards and extreme weather events.

**Dimitris N. Trakas** (S'16) received his diploma in Electrical and Computers Engineering from National Technical University of Athens (NTUA), Greece in 2009, and the Master of Sciences in Energy Production and Management from NTUA in 2011. He is currently a Ph.D. student at Electric Power Division of NTUA.

His research interests include decentralized control of power systems, power system dynamic security, assessment and enhancement of power systems resilience to natural disasters.

**Pierluigi Mancarella** (M'08–SM'14) received the Ph.D. degree in Electrical Energy Systems from the Politecnico di Torino, Italy, in 2006. After a few years as a Research Associate at Imperial College London, UK, in 2011 Pierluigi joined the University of Manchester, UK, where he is currently a Reader in Future Energy Networks.

Pierluigi's research interests include multi-energy systems modelling, power system integration of low carbon technologies, network investment under uncertainty, and risk and resilience of smart grids. He is author of several books and book chapters and over 200 research papers on those topics.

Pierluigi is an Editor of the IEEE Transactions on Smart Grid, an Associate Editor of the IEEE Systems Journal and of the International Journal of Electrical Power and Energy Systems, and the Chair of the Energy Working Group of the IEEE European Public Policy Initiative.

**Nikos D. Hatziargyriou** (S'80–M'82–SM'90–F'09) is Chairman and CEO of the Hellenic Distribution Network Operator. Since 1984 he is with the Power Division of the Electrical and Computer Engineering Department of the National Technical University of Athens and since 1995 he is full professor in Power Systems. From February 2007 to September 2012, he was Deputy CEO of the Public Power Corporation (PPC) of Greece, responsible for Transmission and Distribution Networks, island DNO and the Center of Testing, Research and Prototyping. He is Fellow Member of IEEE, past Chair of the Power System Dynamic Performance Committee, Distinguished member of CIGRE and past Chair of CIGRE SC C6 "Distribution Systems and Distributed Generation". He is chair of the Advisory Council of the EU Technology Platform on SmartGrids. He has participated in more than 60 R&DD Projects funded by the EC and the industry, he is author of the book "Microgrids: Architectures and Control" and of more than 180 journal publications and 500 conference proceedings papers.